# Joining bits and pieces of reionization history

Dhiraj Kumar Hazra*
*INFN, Sezione di Bologna, via Irnerio 46, 40126 Bologna, Italy*
*INAF OAS Bologna, Osservatorio di Astrofisica e Scienza dello Spazio di Bologna, via Gobetti 101, I-40129 Bologna, Italy*

Daniela Paoletti† and Fabio Finelli‡
*INAF OAS Bologna, Osservatorio di Astrofisica e Scienza dello Spazio di Bologna, via Gobetti 101, I-40129 Bologna, Italy*
*INFN, Sezione di Bologna, via Irnerio 46, 40126 Bologna, Italy*

George F. Smoot§
*AstroParticule et Cosmologie (APC)/Paris Centre for Cosmological Physics,*
*Université Paris Diderot, CNRS, CEA, Observatoire de Paris, Sorbonne Paris Cité University,*
*10, rue Alice Domon et Leonie Duquet, 75205 Paris Cedex 13, France;*
*Institute for Advanced Study & Physics Department,*
*Hong Kong University of Science and Technology, Clear Water Bay, Kowloon, Hong Kong*
*Physics Department and Lawrence Berkeley National Laboratory,*
*University of California, Berkeley, CA 94720, USA*
*Energetic Cosmos Laboratory, Nazarbayev University, Astana, Kazakhstan*

(Dated: April 3, 2019)

Cosmic Microwave Background temperature and polarization anisotropies from Planck have estimated lower value of the optical depth to reionization ($\tau$) compared to WMAP. A significant period in the reionization history, therefore falls within $6 <$ redshift$(z) < 10$ where overlap with the galaxies detected with Hubble Frontier Fields (HFF) program and independent estimation of neutral hydrogen in the inter galactic medium by Lyman-$\alpha$ observations becomes important. This overlap calls for an analysis of cosmic reionization which allows a direct combination of CMB and astrophysical measurements. For the first time we reconstruct reionization histories where the photo-ionization and recombination rates are assumed to be free-form using the Planck CMB (temperature and polarization anisotropies and lensing) and a selection of astrophysical data allowing underlying cosmological parameters to vary. This conservative approach removes model bias, explores degeneracies between reionization and other cosmological parameters in a framework that allows sharp to extended histories of reionization. We find that CMB and astrophysical datasets cannot agree if reionization process is sharp. In this joint estimation, we report a derived conservative constraint $\tau = 0.063^{+0.005\,+0.02}_{-0.013\,-0.017}$ (68.3% and 95% C.L.). We find the duration of reionization, redshift interval between 10% ionization and nearly complete ionization, to be $2.4 < \Delta_z^{\rm reion} < 11.9$ at 95% C.L. We do not obtain any evidences for double reionization; and within allowed possibilities we find monotonic histories are preferred over other scenarios when CMB and astrophysical data are combined.

PACS numbers: 98.80.Cq



## INTRODUCTION

The two cosmic transitions between ionized and neutral state for the hydrogen atom are imprinted in key astrophysical and cosmological observations. The first transition from ionized plasma to neutral state for atoms, *cosmological recombination* occurred around 13.8 billion of years ago (or equivalently at a redshift $z \sim 1100$). After half a billion years, the hydrogen became ionized again during *cosmic reionization*, which followed the so called dark ages. Evidence for cosmic reionization comes from astrophysical measurements, such as the Gunn-Peterson test in high redshift quasars or the declining visibility of Lyman-$\alpha$ high redshift galaxies, and from cosmological observations as the large angular scale polarization pattern of CMB anisotropies. While astrophysical measurements mostly encode the central stage and the completion of cosmic reionization, the CMB anisotropy pattern is sensitive to its duration through the integrated optical depth $\tau$, and marginally to its early stage.

The recent determination of the optical depth from Planck by assuming a nearly instantaneous transition for the ionization fraction [1–6] has revealed a preference for lower values ($\tau_{\rm Planck\ 2015} = 0.063 \pm 0.014$) compared to WMAP releases owing to the understanding of the Galactic dust contamination to microwave polarization at large angular scales. Recent works demonstrate that star forming galaxies detected till $z \simeq 10$ as a source of reionization offer a consistent scenario with this optical depth [7]. Observation of star forming galaxies at high redshifts ($z \sim 6 - 10$), mainly with recent six cluster observations (Abell 2744, MACSJ0416, MACSJ0717, MACSJ1149, AbellS1063, Abell370) by Hubble Frontier Fields program [8–10] upto a limiting AB magnitude of 29, provides shape of UV luminosity densities that determine the ionizing photon emission history. On the other

hand, Lyman-$\alpha$ observations such as the Gunn-Peterson optical depth [11, 12], damping wings in quasar spectra [13], Lyman-$\alpha$ emission in galaxies [14–19], ionized near zone around high redshift quasars [20, 21] provide measurement of remaining neutral hydrogen in the intergalactic medium (IGM) between redshift $5-8$. Redshift overlap of HFF and Lyman-$\alpha$ observation and available CMB temperature and polarization power spectrum from Planck calls for a joint analysis in a model independent framework. Since physics describing cosmic reionization is partially degenerate with cosmological parameters [22], it is important to perform this analysis by allowing the underlying cosmological model to vary as well (see [7, 23–31] for previous works in which all but the reionization parameters are kept fixed).

In this Letter we perform for the first time a joint analysis using general reionization history assuming flat $\Lambda$CDM model by using the Planck publicly available data in temperature, polarization angular power spectrum and lensing [2, 32], complete HFF data compilation for UV luminosity densities and neutral hydrogen fraction measurements from Lyman-$\alpha$ observations. To directly constrain ionizing sources, we use solutions of ionization equation of hydrogen with allowing freedom in ionization and recombination rates as the histories instead of conventional free-electron fraction parametrization [22, 33–39]. Our analysis removes the model bias by using this generic construct. At the same time use of complete CMB data and freedom in the cosmological parameters exploits the degeneracies and provide conservative constraints.

## CONSTRUCTION OF REIONIZATION HISTORY: THE FRAMEWORK

In order to model the reionization history in this analysis, we directly solve the reionization equation for the volume filling factor of ionized regions:

$$\frac{dQ_{\rm HII}}{dt} = \frac{\dot{n}_{\rm ion}}{\langle n_{\rm H}\rangle} - \frac{Q_{\rm HII}}{t_{\rm rec}}, \qquad (1)$$

where the source term $\dot{n}_{\rm ion}$ is the ionizing photon production rate and is defined by the product of the UV luminosity density ($\rho_{\rm UV}$), the photon production efficiency ($\xi_{\rm ion}$) and the escape fraction ($f_{\rm esc}$). We keep the magnitude averaged product $\log_{10}\langle f_{\rm esc}\xi_{\rm ion}\rangle = 24.85$ which is consistent with other analyses [7, 28, 29, 40]. $\rho_{\rm UV}$ is defined in different nodes and the nodes are allowed to vary between the conservative window of reionization, $z = 5.5 - 30$. The recombination time is usually defined as $t_{\rm rec} = 1/\left[C_{\rm HII}\alpha_{\rm B}(T)(1+Y_p/(4X_p))\langle n_{\rm H}\rangle(1+z)^3\right]$ using the clumping factor ($C_{\rm HII}$), recombination coefficient ($\alpha_{\rm B}(T)$), density of hydrogen atom ($\langle n_{\rm H}\rangle$) and hydrogen ($X_p$) and helium abundances ($Y_p$). However in this work, instead of using this analytical form we allow $t_{\rm rec}$ to be free as well in the same redshifts where $\rho_{\rm UV}$'s are defined. Different nodes are connected using Piecewise Cubic Hermite Interpolating Polynomial (PCHIP). Fixed nodes are located at $z = 0, 5.5$ and 30 and values of source and recombination terms are fixed to be consistent to best fit logarithmic double power law (see, Eq. (39) of [28]) and also consistent with [41]. However as we allow the intermediate source and recombination terms to be free, values at fixed nodes do not limit our generic construct. We allow upto three nodes in this moving-bin reconstruction denoted as $B1$, $B2$ and $B3$ respectively and each node comes with three parameters, namely, the redshift ($z_{\rm int}$), UV luminosity density ($\rho_{\rm UV}^{\rm int}$) and the ratio of the recombination and the source term ($R^{\rm int}$). For a minimal construct we also consider $B0$ where we impose at $z = z_{\rm int}$, $\dot{n}_{\rm ion}t_{\rm rec} = \langle n_{\rm H}\rangle$. The optical depth is given by the integral from onset of reionization ($z_{\rm begin}$) till today : $\tau = \int_0^{z_{\rm begin}} \frac{c(1+z)^2}{H(z)} Q_{\rm HII}(z)\sigma_{\rm Thomson}\langle n_{\rm H}\rangle(1+\frac{Y_p}{4X_p})$, where $\sigma_{\rm Thomson}$ is the Thomson scattering cross-section. We fuse our integrator with CAMB maintaining the standard treatment for Helium reionization. Our free form reconstruction allows a wide prior on the history of reionization and its physical parameters can be obtained in a post-processing.

## DATASETS AND PRIORS

Three different datasets has been used in this work. For CMB we use the latest publicly available 2015 likelihoods in temperature, polarization and lensing (hereafter P15) [2, 32]. We use the full angular power spectrum data instead of a prior on optical depth, because the constraint on $\tau$ is model dependent [36, 37, 39, 42–44] and there exist non-negligible correlations between reionization history and other cosmological parameters [22]. For UV luminosity density, we use [7, 45] data spanning $z \sim 6 - 11$ (denoted by UV) which were derived from Hubble Frontier Fields [9, 46] observations. The density is obtained by integrating the UV luminosity function by fitting Schechter function till a truncation magnitude of $-17$ [1]. We also use direct $Q_{\rm HII}$ constraints (denoted by QHII) from Gunn-Peterson optical depth data [12], damping wings of quasars [13] and Lyman-$\alpha$ emission from galaxies [14]. These data cover a redshift range of $6-8$ and thereby overlap with the UV density. We have results for three data combinations, *viz.* P15, P15+UV and P15+UV+QHII. Only for B3 we do not explore P15-only constraints owing to the inability of CMB to provide reasonable constraints in vastly degenerate parameter space. For B0 and B1 the intermediate redshift is allowed to vary between the entire range $z = 5.5-30$. For

[1] We use the data compiled by Ishigaki *et. al* (2018)

B2, we allow $z^1_{\rm int}$ to vary between $z = 5.5-12$ to incorporate the UV data range and $z^2_{\rm int}$ between $z = 12-30$ to explore the tail. For B3, $z^1_{\rm int}$, $z^2_{\rm int}$ and $z^3_{\rm int}$ move within $5.5-8$, $8-12$ and $12-30$ respectively. The redshift ranges of B2 nodes are chosen in a way that the UV data can constrain the source term variation in the first node and the P15 constrains the tail end of the histories by constraining the integrated optical depth. Similarly, first two nodes of B3 are designed to capture any suppression or break in the power of the luminosity densities and the final node ranges as in the case of B2. Note that $\tau$ is a derived parameter in our framework. We allow $\Omega_{\rm b}h^2$, $\Omega_{\rm CDM}h^2$, $\theta$, $A_{\rm s}$, $n_{\rm s}$ and nuisance and calibration parameters in Planck likelihood to vary.

## CONSTRAINTS AND CONCORDANCES

We obtain constraints using P15, P15+UV and P15+UV+QHII in single node minimal (B0), single node (B1), 2 nodes (B2) cases and P15+UV and P15+UV+QHII in three nodes (B3) case. In Table I we

| Model/ Data | P15 | P15+UV | P15+UV+QHII |
|---|---|---|---|
| B0 (1 node) varying source $\dot{n}_{\rm ion}$ only | 6476.7<br>$0.059^{+0.026}_{-0.024}$ | 6479.3<br>$0.049 \pm 0.002$ | 6485.6<br>$0.054 \pm 0.0015$ |
| B1 (1 node) | 6475.9<br>$0.062^{+0.027}_{-0.028}$ | 6479.1<br>$0.049 \pm 0.002$ | 6480.8<br>$0.053 \pm 0.003$ |
| B2 (2 nodes) | 6476.5<br>$0.064 \pm 0.03$ | 6478.6<br>$0.051^{+0.02}_{-0.013}$ | 6477.1<br>$0.06 \pm 0.012$ |
| B3 (3 nodes) | - | 6477.7<br>$0.057^{+0.03}_{-0.02}$ | 6477.8<br>$0.063^{+0.02}_{-0.017}$ |

TABLE I: Best fit $-\ln\mathcal{L}$ from MCMC and the bounds on the optical depth in our model for different data combinations. P15 for B3 has not been analyzed as the increased degeneracy with 3 nodes does not allow reasonable constraint from P15. In each cell, top row indicates best $-\ln\mathcal{L}$ and bottom row contains $\tau$.

provide the $\chi^2_{\rm eff}/2 = -\ln\mathcal{L}$ and $\tau$ (with 95% uncertainties) in top and bottom rows in each cell respectively. It can be readily identified for B0 and B1, that allow monotonic histories, $\tau$ can be constrained with more than one order of magnitude better precision when astrophysical data from UV and UV+QHII are used with Planck compared to P15. In all the cases, mean values of optical depth increase when QHII constraints are used as they rule out incomplete reionization histories by $z \sim 6$ and thereby discard low $\tau$ values. With the increase in degeneracy in B2, addition of UV and UV+QHII only improves the constraint by 50% compared to P15. Since in B2, the node that spans $z = 12-30$ is only constrained by P15, constraint in the direction of higher optical depth gets worse. In the combined analysis, as expected we find weaker constraints in B3 compared to B2. In this joint constraint, interestingly the measured optical depth for all cases remain completely consistent with Planck 2018 results. In [30], using five (four star formation history parameters and clumping factor) and six (allowing $f_{\rm esc}$ to vary alongside) parameters, the authors report the standard deviation of $\tau$ to be 0.0019 and 0.002 respectively, when all datasets are used. Note that in B2, that allows 6 parameters to describe the reionization, we find the 95% error to be $\sim 0.012$ which is three times wider compared to [30]. The constraints become more conservative as our reconstructions allow more flexibilities compared to reionization history parametrization. In Fig. 1 we plot the samples from the MCMC analyses. After removing the burn-in samples we randomly select 500 samples and plot $Q_{\rm HII}$ (top row) for all the cases. While B0 produces monotonic power law reionization histories, B1 allows extended and step like histories. B2 and B3 with extra nodes provide the scopes for non-monotonic and complex histories. P15 mainly constrains the integrated optical depth, therefore the ionization histories are not well constrained in all three cases (B0, B1 and B2). UV luminosity density constraints allow only a small subset of histories from P15 and the derived bounds on $\tau$ improve significantly in P15+UV. Plots indicate strong preference of monotonic ionization histories compared to other complex processes. Table I shows a $\chi^2_{\rm eff}$ difference of $\sim 10$ between B0 and B1 in the expense of one extra parameter which rules out B0. With increased number of parameters, B1, B2 and B3 resolve this tension and we find sufficient overlap between samples. The $\chi^2_{\rm eff}$ difference also becomes insignificant for more than two nodes [2]. In the middle row of same figure, we plot corresponding source term, $\rho_{\rm UV}$ as a function of redshift and on top we display the Ishigaki *et. al.* (2018) data points used. The luminosity densities at higher redshifts for B2 and B3 are not constrained well and therefore we plot samples only till $z = 12$. The importance of using the $\rho_{\rm UV}$ constraints is evident as the sparseness of samples is significantly reduced. When QHII datasets are used, we find a preference of less red tilt in the $\rho_{\rm UV}$ samples compared to P15+UV. In the bottom row of the same figure we plot the marginalized constraints on the optical depth. In all the cases the dominance of astrophysical datasets over CMB is evident. $\tau$ from P15+UV and P15+UV+QHII, as expected agree well in all cases except B0. With increase in nodes, we find bounds on $\tau$ are significantly relaxed in B2 and B3 as the tail end of the history is only constrained with CMB which in this free form framework provides higher flexibilities (see top row

[2] Note that in some cases a model with more nodes finds $\chi^2_{\rm eff}$ which is $\sim 1$ worse than a model with less nodes. Since MCMC does not converge to a global best fit a minimizer routine is required. We do not use any global minimizer routine here as we mainly aim for the posterior probabilities.

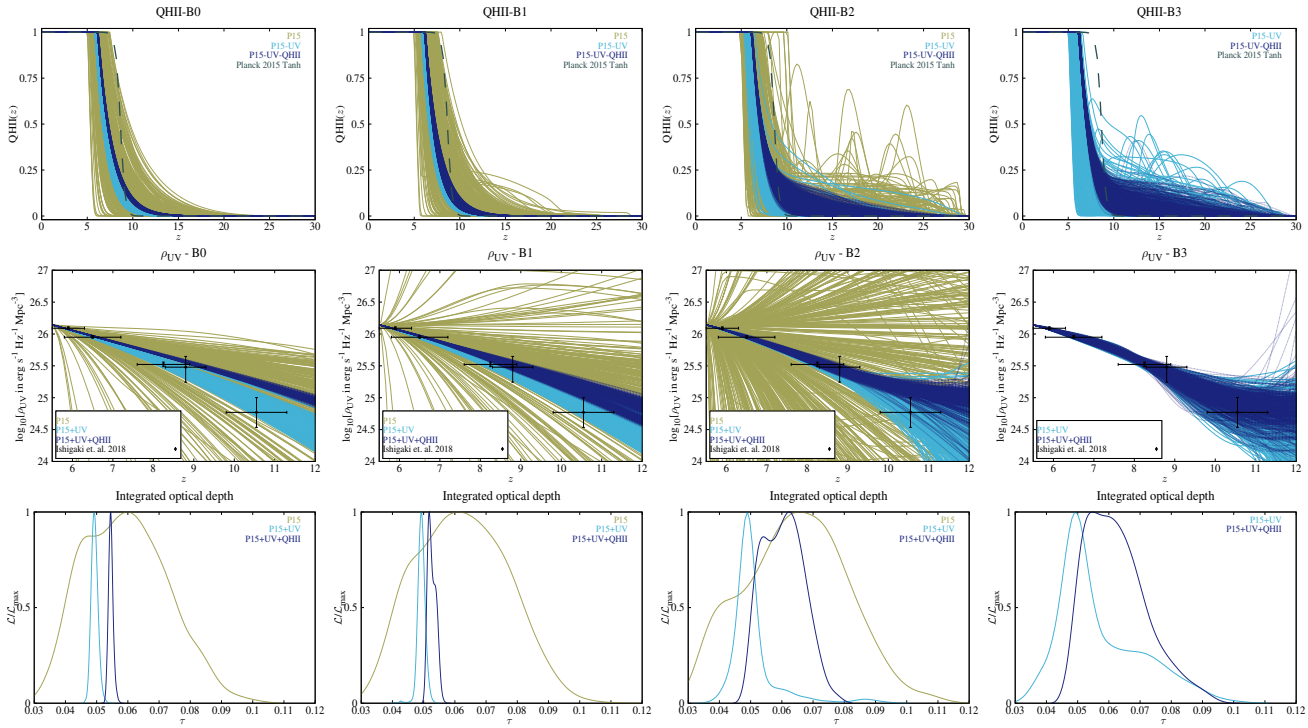


FIG. 1: [Left to right]: Results for single node minimal (B0), single node (B1), two nodes (B2) and three nodes (B3) reconstructions respectively. Planck best fit for Tanh reionization is plotted in dashed gray. [Top]: The volume filling factor as a function of redshift. 500 random samples are plotted from the complete MCMC samples. [Middle]: UV luminosity density with the Ishigaki *et. al.* compiled data. Here we plot only till $z = 12$. [Bottom]: Marginalized probability distribution function of $\tau$. It is evident from the plots that a sharp history of reionization can not make all three datasets agree.

of the same figure). In Fig. 2 we plot the constraints on ionizing photon production rate ($\dot{n}_{\rm ion}$) as a function of redshift for P15+UV and P15+UV+QHII in B1, B2 and B3 cases as they provide consistent histories in these two combinations. Note that only with one flexible node, we can reconstruct the bounds on $\dot{n}_{\rm ion}$ in the entire epoch. In B1 although we have limited overlap of contours in these two combinations, B2 and B3 show complete consistency at all redshifts. Note that in the plots the redshift and $\dot{n}_{\rm ion}$ ranges are kept different for better visibility. We find correlations between other background cosmological parameters $(A_{\rm s}, n_{\rm s}, \Omega_{\rm m}, H_0)$ with reionization optical depth. With spectral index such correlation has already been explored in [22]. Fig. 3 captures that correlation in our reionization framework B1 (left) and B2 (right). We find in the case of monotonic histories generated by B1, $\tau$ and $n_{\rm s}$ are correlated when only CMB is used. Astrophysical data break this degeneracy and provide tighter constraint on the reionization histories and therefore on $\tau$. However, B2 allows non-monotonic histories and also allow highly extended histories of ionization leading to higher values of optical depth. As we mentioned before, the tail end is only constrained by CMB which allows for higher $\tau$ values and therefore, even when UV and QHII are used, residual degeneracies exist in the high $n_{\rm s} - \tau$ direction. In Fig. 4, we plot the 68.3% and 95% C.L. on the reionization histories for all the reconstructions using P15+UV+QHII combination. On top of the bounds, we plot $Q_{\rm HII}$ data points from different observations. Note that we have not used all these points in our analysis. We however, find that constraints on the reconstructed history are consistent with other observations. In the joint analysis, we find tight constraints on the duration of reionization ($\Delta_z^{\rm reion}$ [3]). We define $z_{10}$ as the redshift for 10% ionization. For P15+UV+QHII data combination we find $9.5 < z_{10} < 10$, $8.9 < z_{10} < 9.9$, $8.8 < z_{10} < 14.3$ and $8.4 < z_{10} < 17.9$ for B0, B1, B2 and B3 respectively at 95% C.L. From the plot while it seems that the Lyman-$\alpha$ emission data from [14] is dragging the bounds to a fine tuned region and thereby tightening $\Delta_z^{\rm reion}$ constraints, it is not indeed true. We post processed the B3 chains from P15+UV with added $Q_{\rm HII}$ constraint only at $z = 6.1$ and find marginal changes in duration ($2.1 < \Delta_z^{\rm reion} < 11.1$). It is the combination of $Q_{\rm HII}$ at $z = 6.1$ and the non-instantaneous decrease in $\rho_{\rm UV}$ data that leads to this lower bound on the duration of reionization. In this framework we also reconstruct

[3] redshift difference between 10% and nearly complete ionization ($z_{100}$)

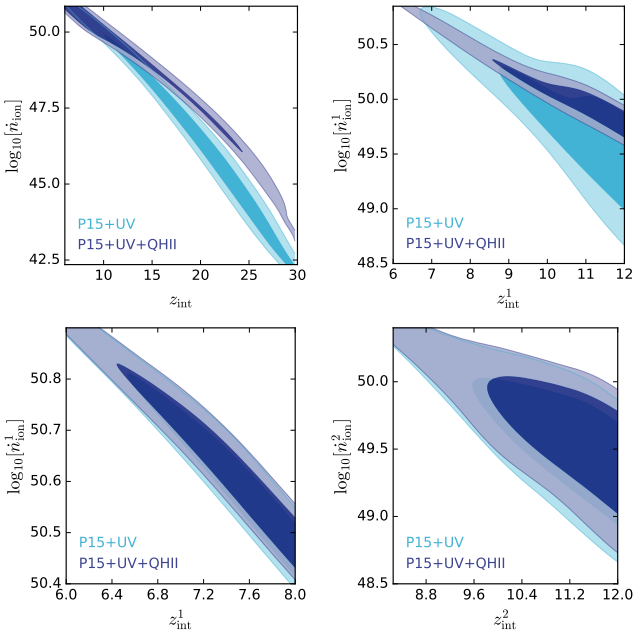


FIG. 2: Constraints on the ionizing photon production date, $\dot{n}_{\rm ion}$ as a function of redshift in single node (B1), 2 nodes (B2) and three nodes (B3) reconstructions using P15+UV and P15+UV+QHII combination. For B1 (top left) we plot between $6 < z < 30$. For B2 (top right) we only plot between $6 < z < 12$, within the prior range of the first node. For B3 (bottom) we only plot between $6 < z < 8$ and $8 < z < 12$, within the prior range of the first two nodes.

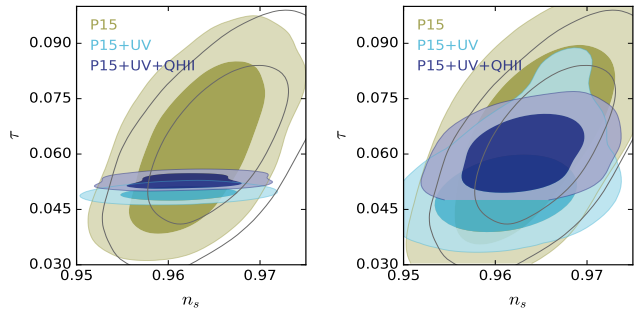


FIG. 3: Degeneracies between the spectral index ($n_{\rm s}$) and the optical depth ($\tau$) in single node (B1: left) and two nodes reconstructions (B2: right). The correlation between these two parameters can be broken to a significant extent when astrophysical data are used. However, complex histories that B2 offers, will still have some residual correlation even in a joint study. The empty gray contours correspond to baseline Tanh reionization for P15.

the clumping factor at different redshifts since the term $t_{\rm rec}$ is dependent on clumping factor and recombination coefficient in the conventional framework. Here assuming IGM temperature to be $2\times10^4 K$, we find $C_{\rm HII} \lesssim 3$ within $6 < z < 8$ and monotonically increasing with decrease in redshift. This result is completely consistent with parametric $C_{\rm HII} = 2.9\left[\frac{1+z}{6}\right]^{-1.1}$ fit to simulation [47] . We

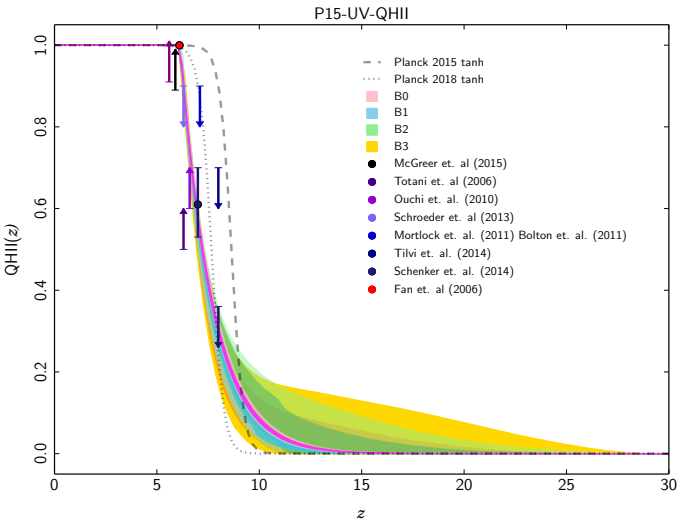


FIG. 4: 68.3% and 95% C.L. on $Q_{\rm HII}$ as a function of redshift in four different cases considered. Data points and limits are also plotted. In dashed and dotted lines best fit Tanh model for Planck 2015 and Planck 2018 are plotted. Note that the sharp change offered by Tanh model does not address $Q_{\rm HII}$ limits efficiently. The free form reconstruction provides a family of reionization histories that are in concordance with both CMB and astrophysical datasets.

expect that this bound may further relax if $\langle f_{\rm esc}\xi_{\rm ion}\rangle$ is allowed to be free [4]. UV luminosity densities obtained from different truncation magnitudes may also degrade the constraints to some extent.

## CONCLUSION

In this analysis we reconstruct the history of reionization using one to 8 extra parameters compared to the conventional Tanh parametrization in the free electron fraction with only $\tau$ or $z_{\rm re}$ as free parameter. The parameters in our free form history reconstruction are the redshifts at the nodes, the source term ($\dot{n}_{\rm ion}$) and the recombination time $t_{\rm rec}$ at those redshifts. Our framework allows sharp to highly extended reionization histories that also involves non-monotonic changes in the ionization fraction. We use CMB and selected astrophysical data to reconstruct the evolution of the ionization fraction.

Below we summarize the main results of our analysis:

1. A joint analysis that includes Planck 2015 data, UV

[4] $\langle f_{\rm esc}\xi_{\rm ion}\rangle$ is not allowed to vary in our work as it is highly degenerate with the clumping factor; as we keep the recombination part to be free form and allow other cosmological parameters to vary the degeneracy will increase severely to obtain any reasonable bounds on the reconstruction.

luminosity density integrated upto -17 magnitude and Lyman-$\alpha$ observations, does not allow sharp reionization histories. Both P15+UV and P15+UV+QHII combinations rule out near instantaneous reionization in all the cases we have considered, *i.e.* allowing upto three nodes with 9 parameters in the reionization histories. From minimal model (B0) to one moving node (B1), that allows one extra parameter by freeing recombination rate, we find $\sim 10$ improvement in $\chi^2_{\rm eff}$ for P15+UV+QHII data combination. We find no support in constructing the history beyond 2 nodes reconstruction. We report constraints at 95% C.L. on $z_{10}$ (redshift when reionization is 10% complete) to be $9.5 < z_{10} < 10$ (one node with varying only ionizing source term), $8.9 < z_{10} < 9.9$ (one node), $8.8 < z_{10} < 14.3$ (two nodes) and $8.4 < z_{10} < 17.9$ (three nodes). Therefore the duration of reionization is constrained to be $2.4 < \Delta_z^{\rm reion} < 11.9$ in the conservative case. Post-processing the chains from P15+UV using just the constraint of completion of reionization at $z \sim 6$ reveals $2.1 < \Delta_z^{\rm reion} < 11.1$.

2. There are no evidences for non-monotonic or multi-step reionization histories, though these histories are neither excluded by the data. Note that one node, by construction allows only monotonic histories while two and three nodes can allow one and two intermediate breaks in the increasing ionization fraction. Allowing all these possibilities, we find P15+UV+QHII combination favors monotonic ionization histories over others in both two and three node reconstructions.

3. UV luminosity density provide tighter bounds on the Thomson scattering optical depth compared to Planck 2015 datasets. In the most conservative case with three nodes, the combined datasets P15+UV+QHII constrain $\tau = 0.063^{+0.02}_{-0.017}$ at 95% C.L.

4. Under our reconstruction framework, the minimal model does not provide a reasonable fit to the combined CMB data from Planck, UV luminosity density compilation by Ishigaki *et. al.* 2018 and neutral Hydrogen fraction measurements from Lyman-$\alpha$ observations. Extending the model by adding at least one extra parameter ameliorates this tension. As mentioned in the first point of our conclusion, we find significant improvement with only one extra parameter.

5. In this free form reionization history reconstruction using P15+UV+QHII combination, post-process of the samples reveals that clumping factor $C_{\rm HII} \lesssim 3$ within redshift $6-8$, assuming a IGM temperature of 20000K. A variation in $\log_{10}\langle f_{\rm esc}\xi_{\rm ion}\rangle$ will allow a wider range in $C_{\rm HII}$ which is beyond the scope of this analysis.

6. We find that for simple monotonic models that can be described by a single intermediate node, degeneracies between background cosmological parameters and reionization history parameters can be lifted completely with astrophysical data. Complex models however, allow certain histories that are beyond the reach of astrophysical observations and can be only constrained by integrated optical depth. In such cases residual degeneracies persist in the higher $\tau$ direction even in a joint analysis.

Our analysis opens up to conservative constraints which include astrophysical measurements with CMB on how reionization evolved. Use of complete CMB angular power spectrum and lensing data in this framework removes model bias, explores the complete degeneracies with background parameters and also allows astrophysical data to be used that breaks the degeneracies to a significant extent. With the release of Planck 2018 likelihood, this framework can be used more efficiently with competing constraints from CMB and astrophysical data.

### Acknowledgments

The authors would like to acknowledge the use of APC cluster (https://www.apc.univ-paris7.fr/FACeWiki/pmwiki.php?n=Apc-cluster.Apc-cluster) and INAF OAS Bologna cluster. The authors thank Masami Ouchi and Masafumi Ishigaki for providing their UV luminosity density data compilation. DKH would like to thank Sourav Mitra for important discussions. DP and FF acknowledge financial support by ASI Grant 2016-24-H.0 and partial financial support by the ASI/INAF Agreement I/072/09/0 for the Planck LFI Activity of Phase E2. GFS acknowledge Laboratoire APC-PCCP, Université Paris Diderot and Sorbonne Paris Cité (DXCACHEXGS) and also the financial support of the UnivEarthS Labex program at Sorbonne Paris Cité (ANR-10-LABX-0023 and ANR-11-IDEX-0005-02).

* Electronic address: hazra@bo.infn.it
† Electronic address: daniela.paoletti@inaf.it
‡ Electronic address: fabio.finelli@inaf.it
§ Electronic address: gfsmoot@lbl.gov

[1] P. A. R. Ade et al. (Planck), Astron. Astrophys. **594**, A13 (2016), 1502.01589.
[2] N. Aghanim et al. (Planck), Astron. Astrophys. **594**, A11 (2016), 1507.02704.
[3] R. Adam et al. (Planck), Astron. Astrophys. **596**, A108 (2016), 1605.03507.
[4] N. Aghanim et al. (Planck), Astron. Astrophys. **596**, A107 (2016), 1605.02985.
[5] M. Lattanzi, C. Burigana, M. Gerbino, A. Gruppuso, N. Mandolesi, P. Natoli, G. Polenta, L. Salvati, and T. Trombetti, JCAP **1702**, 041 (2017), 1611.01123.
[6] N. Aghanim et al. (Planck) (2018), 1807.06209.

[7] M. Ishigaki, R. Kawamata, M. Ouchi, M. Oguri, K. Shimasaku, and Y. Ono, Astrophys. J. **854**, 73 (2018), 1702.04867.

[8] D. Coe, L. Bradley, and A. Zitrin, Astrophys. J. **800**, 84 (2015), 1405.0011.

[9] J. M. Lotz, A. Koekemoer, D. Coe, N. Grogin, P. Capak, J. Mack, J. Anderson, R. Avila, E. A. Barker, D. Borncamp, et al., Astrophys. J. **837**, 97 (2017), 1605.06567.

[10] R. C. Livermore, S. L. Finkelstein, and J. M. Lotz, Astrophys. J. **835**, 113 (2017), 1604.06799.

[11] X.-H. Fan, C. L. Carilli, and B. G. Keating, Ann. Rev. Astron. Astrophys. **44**, 415 (2006), astro-ph/0602375.

[12] X.-H. Fan, M. A. Strauss, R. H. Becker, R. L. White, J. E. Gunn, G. R. Knapp, G. T. Richards, D. P. Schneider, J. Brinkmann, and M. Fukugita, Astron. J. **132**, 117 (2006), astro-ph/0512082.

[13] J. Schroeder, A. Mesinger, and Z. Haiman, Mon. Not. Roy. Astron. Soc. **428**, 3058 (2013), 1204.2838.

[14] M. A. Schenker, R. S. Ellis, N. P. Konidaris, and D. P. Stark, Astrophys. J. **795**, 20 (2014), 1404.4632.

[15] Y. Ono, M. Ouchi, B. Mobasher, M. Dickinson, K. Penner, K. Shimasaku, B. J. Weiner, J. S. Kartaltepe, K. Nakajima, H. Nayyeri, et al., Astrophys. J. **744**, 83 (2012), 1107.3159.

[16] J. Caruana, A. J. Bunker, S. M. Wilkins, E. R. Stanway, S. Lorenzoni, M. J. Jarvis, and H. Ebert, Mon. Not. Roy. Astron. Soc. **443**, 2831 (2014), 1311.0057.

[17] L. Pentericci et al., Astrophys. J. **793**, 113 (2014), 1403.5466.

[18] E. Sobacchi and A. Mesinger, Mon. Not. Roy. Astron. Soc. **453**, 1843 (2015), 1505.02787.

[19] V. Tilvi, C. Papovich, S. L. Finkelstein, J. Long, M. Song, M. Dickinson, H. Ferguson, A. M. Koekemoer, M. Giavalisco, and B. Mobasher, Astrophys. J. **794**, 5 (2014), 1405.4869.

[20] D. J. Mortlock, S. J. Warren, B. P. Venemans, M. Patel, P. C. Hewett, R. G. McMahon, C. Simpson, T. Theuns, E. A. Gonzáles-Solares, A. Adamson, et al., Nature (London) **474**, 616 (2011), 1106.6088.

[21] J. S. Bolton, M. G. Haehnelt, S. J. Warren, P. C. Hewett, D. J. Mortlock, B. P. Venemans, R. G. McMahon, and C. Simpson, Mon. Not. Roy. Astron. Soc. **416**, L70 (2011), 1106.6089.

[22] D. K. Hazra, D. Paoletti, F. Finelli, and G. F. Smoot, JCAP **1809**, 016 (2018), 1807.05435.

[23] B. E. Robertson, R. S. Ellis, J. S. Dunlop, R. J. McLure, and D. P. Stark, Nature (London) **468**, 49 (2010), 1011.0727.

[24] S. Mitra, T. R. Choudhury, and A. Ferrara, Mon. Not. Roy. Astron. Soc. **419**, 1480 (2012), 1106.4034.

[25] S. Mitra, T. R. Choudhury, and A. Ferrara, Mon. Not. Roy. Astron. Soc. **454**, L76 (2015), 1505.05507.

[26] R. J. Bouwens, G. D. Illingworth, P. A. Oesch, J. Caruana, B. Holwerda, R. Smit, and S. Wilkins, Astrophys. J. **811**, 140 (2015), 1503.08228.

[27] B. E. Robertson, R. S. Ellis, S. R. Furlanetto, and J. S. Dunlop, Astrophys. J. **802**, L19 (2015), 1502.02024.

[28] M. Ishigaki, R. Kawamata, M. Ouchi, M. Oguri, K. Shimasaku, and Y. Ono, Astrophys. J. **799**, 12 (2015), 1408.6903.

[29] L. C. Price, H. Trac, and R. Cen (2016), 1605.03970.

[30] A. Gorce, M. Douspis, N. Aghanim, and M. Langer, Astron. Astrophys. **616**, A113 (2018), [Astron. Astrophys.616,A113(2018)], 1710.04152.

[31] S. Mitra, T. R. Choudhury, and A. Ferrara, Mon. Not. Roy. Astron. Soc. **473**, 1416 (2018), 1606.02719.

[32] P. A. R. Ade et al. (Planck), Astron. Astrophys. **594**, A15 (2016), 1502.01591.

[33] W. Hu and G. P. Holder, Phys. Rev. **D68**, 023001 (2003), astro-ph/0303400.

[34] M. J. Mortonson and W. Hu, Astrophys. J. **672**, 737 (2008), 0705.1132.

[35] M. Douspis, N. Aghanim, S. Ili, and M. Langer, Astron. Astrophys. **580**, L4 (2015), 1509.02785.

[36] D. K. Hazra and G. F. Smoot, JCAP **1711**, 028 (2017), 1708.04913.

[37] G. Obied, C. Dvorkin, C. Heinrich, W. Hu, and V. Miranda, Phys. Rev. **D98**, 043518 (2018), 1803.01858.

[38] C. Heinrich and W. Hu, Phys. Rev. **D98**, 063514 (2018), 1802.00791.

[39] P. Villanueva-Domingo, S. Gariazzo, N. Y. Gnedin, and O. Mena, JCAP **1804**, 024 (2018), 1712.02807.

[40] P. Madau, Astrophys. J. **851**, 50 (2017), 1710.07636.

[41] G. D. Becker and J. S. Bolton, Mon. Not. Roy. Astron. Soc. **436**, 1023 (2013), 1307.2259.

[42] D. K. Hazra, D. Paoletti, M. Ballardini, F. Finelli, A. Shafieloo, G. F. Smoot, and A. A. Starobinsky, JCAP **1802**, 017 (2018), 1710.01205.

[43] C. Heinrich and W. Hu, Phys. Rev. **D98**, 063514 (2018), 1802.00791.

[44] M. Millea and F. Bouchet, Astron. Astrophys. **617**, A96 (2018), 1804.08476.

[45] R. J. Bouwens et al., Astrophys. J. **803**, 34 (2015), 1403.4295.

[46] *Hubble space telescope frontier fields*, http://www.stsci.edu/hst/campaigns/frontier-fields/.

[47] J. M. Shull, A. Harness, M. Trenti, and B. D. Smith, Astrophys. J. **747**, 100 (2012).